Chemical Science

ROYAL SOCIETY OF CHEMISTRY

EDGE ARTICLE

View Article Online
View Journal

Cite this: DOI: 10.1039/d5sc07228j

All publication charges for this article have been paid for by the Royal Society of Chemistry

Synergistic diselenide/guanidine catalyzed dehydrophosphorylation of 2-nitrobenzhydrols to access C-stereogenic phosphinates

Jin-Yu Gong,†[a] Pan-Pan Zhou,†[a] Yu-Hao Qiao,[a] Zhi-Chao Qi,[a] Qian-Ming Zuo,[a] Qing-Xia Fang[a] and Shang-Dong Yang *[ab]

Received 18th September 2025
Accepted 12th March 2026

DOI: 10.1039/d5sc07228j

rsc.li/chemical-science

The development of a catalytic and mild variant of the Atherton–Todd reaction for the synthesis of chiral phosphorus-containing compounds presents substantial challenges. Herein, we report a method for accessing C-stereogenic phosphinates enabled by a synergistic diselenide/chiral guanidine catalytic system. This method avoids stoichiometric halogenating reagents, generating water as the sole byproduct. Mechanistic studies reveal that the electron-deficient diselenide catalyst serves as a recyclable alternative for halogenating agents, while the chiral guanidine activates the alcohol *via* Brønsted base catalysis. This strategy effectively achieves the kinetic resolution of secondary alcohols with similar steric substituents, offering a sustainable strategy to access phosphinates with stereogenic benzhydryl groups.

Introduction

Organophosphinates, as a pivotal class of compounds containing phosphorus–oxygen bonds, have attracted substantial attention due to their versatile applications in pharmaceuticals,[1] agrochemicals,[2] and organic synthesis.[3] Conventional approaches for the synthesis of these compounds rely on the reaction between sensitive phosphoryl halides and alcohols or phenols. The Atherton–Todd (A–T) reaction offers a practical alternative by generating these sensitive electrophiles *in situ* from P(O)–H compounds upon treatment with stoichiometric halogenating agents and a base.[4] Building upon this foundation, early improvements employed iodide/oxidant systems to expand the scope and practicality of this approach.[5] More recently, Tf_2O-mediated process has been introduced for the generation of electrophilic phosphorus species.[6] (Fig. 1A).

While various efficient strategies have been established for the Atherton–Todd-type (A–T-type) reaction, the CCl_4-mediated approach has uniquely proven applicable to the synthesis of chiral phosphorus-containing compounds in recent years (Fig. 1B). In 2019, Colobert and colleagues developed a diastereoselective Atherton–Todd reaction using sulfoxides as chiral auxiliaries to achieve dynamic kinetic resolution of racemic P(O)–H compounds.[7] Subsequently, Wang and coworkers pioneered a catalytic protocol for the enantiodivergent synthesis of atropisomeric biaryls *via* a kinetic resolution process, guided by dipeptide-phosphonium salt-catalyzed Atherton–Todd reactions.[8] On this basis, they further expanded the scope of chiral quaternary phosphonium salts catalysis, accessing sulfur-stereogenic sulfoximines[9] and axially chiral phosphate-containing olefins.[10] However, these advanced protocols still depend on stoichiometric CCl_4, which

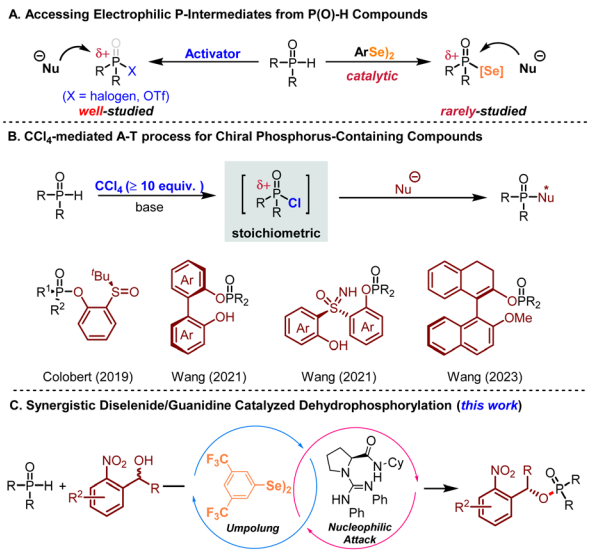

Fig. 1 Dehydrophosphorylation for chiral phosphorus-containing compounds.

[a]State Key Laboratory of Natural Product Chemistry, College of Chemistry and Chemical Engineering, Lanzhou University, 222 South Tianshui Road, Lanzhou 730000, China. E-mail: yangshd@lzu.edu.cn

[b]State Key Laboratory of Low Carbon Catalysis and Carbon Dioxide Utilization, Lanzhou Institute of Chemical Physics, Chinese Academy of Sciences, Lanzhou 730000, China

† These two authors contributed equally.

even acts directly as the solvent component in certain protocols (*i.e.*, in large excess). Therefore, the development of a catalytic and mild variant of the Atherton–Todd reaction for accessing chiral phosphorus-containing compounds becomes imperative.

Against this backdrop, diselenide catalysts[11,12] offer a promising solution. Building on our recent studies in chiral diselenide-catalyzed intramolecular enantioselective desymmetrizing cyclization[13] and our ongoing interest in organophosphorus chemistry,[14] we sought to explore the dehydrogenative phosphinoylation of racemic alcohols with P(O)–H compounds for C-stereogenic phosphinates with catalytic amounts of diselenide. Current progress in this dehydrogenative coupling reaction is limited to racemic transformations mediated by electron-deficient aryl diselenide catalysts.[11g] However, extending this protocol to the synthesis of chiral phosphorus-containing compounds remains highly challenging, primarily due to the limited availability of electron-deficient chiral diselenide catalysts.[11h–p] To the best of our knowledge, there are no general methods for the efficient preparation of these chiral diselenide species. Consequently, new catalytic strategies must fundamentally bypass the need for chiral diselenide catalysts. Given the crucial role of base activation in alcohol functionalization, we propose a dual activation strategy combining achiral electron-deficient diselenide catalysts with chiral organo-superbase catalysts.[15] Chiral organo-superbase catalysts serve as bifunctional catalysts that simultaneously mediate base activation and enantioselective control, while the electron-deficient diselenide facilitates the formation of electrophilic phosphorus intermediates from P(O)–H compounds, creating a synergistic interplay to promote dehydrogenative coupling of P(O)–H compounds with 2-nitrobenzhydrols. This synergistic strategy not only circumvents the need for stoichiometric CCl_4 and chiral diselenide catalysts but, more importantly, effectively achieves the challenging kinetic resolution of secondary alcohols bearing substituents of similar steric demand, providing a sustainable route to C-stereogenic phosphinates with water as the sole byproduct (Fig. 1C).

Results and discussion

Optimization of reaction conditions

Compounds featuring a (2-nitrophenyl)methanol scaffold exhibit potent inhibitory activity against PqsD in *Pseudomonas aeruginosa*,[16] and the nitro group of the substrate, as a strong electron-withdrawing group and hydrogen-bonding acceptor, can assist in chiral control while activating the substrate. In light of these considerations, we evaluated the proposed dual

Table 1 Optimization of the catalyst[a]

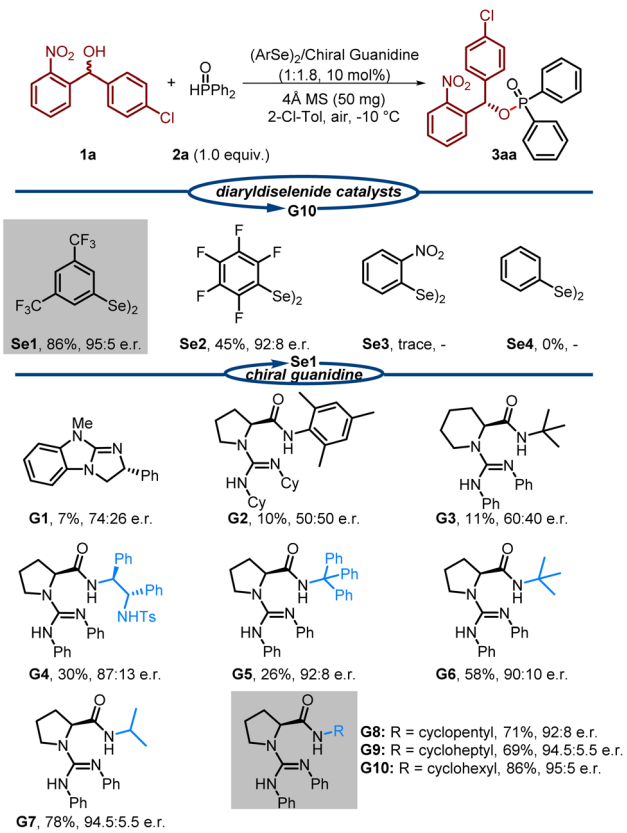

[a] **1a** (0.25 mmol), **2a** (0.1 mmol), $(ArSe)_2$ (10 mol%), **G** (18 mol%), 4 Å MS (50 mg), 2-Cl-Tol (2.5 mL), −10 °C, air. The yields given are isolated yields (based on **2a**). Enantiomeric ratio (e.r.) was determined by HPLC analysis.

activation strategy using achiral diselenide catalysts and chiral guanidine catalysts.[17,18] Using (4-chlorophenyl)(2-nitrophenyl) methanol (**1a**) and diphenylphosphine oxide (**2a**) as model substrates, we conducted the reactions in 2-chlorotoluene at −10 °C with 4 Å molecular sieves as the drying agent, as outlined in Table 1. Fortunately, the reaction proceeded efficiently when using diaryldiselenide with electron-withdrawing groups (**Se1**) and chiral guanidine catalyst (**G10**) with the ratio of 1 : 1.8, delivering the desired phosphinate product **3aa** in 86% yield and a 95 : 5 enantiomeric ratio (e.r.). During this process, we observed that the results were significantly influenced by the amino acid backbone, amide substituents, and amidine substituents of the guanidine catalysts. For instance, the use of bicyclic guanidine (**G1**), dialkyl-substituted catalysts (**G2**), and pipecolinic acid-based catalysts (**G3**) led to poor enantioselectivity and reactivity. Subsequently, we investigated the influence of amide substituents on *N*,*N*-diphenyl-substituted guanidines (**G4–G7**) based on a proline scaffold. A notable improvement was observed when using guanidine **G7**, which features an isopropyl group. Encouraged by these findings, we synthesized a series of guanidines containing cycloalkylamide substituents (**G8–G10**). Remarkably, these guanidines demonstrated significantly enhanced reactivity and enantiocontrol. Among them, the guanidine catalyst with a cyclohexyl amide substituent (**G10**) delivered the best results, as mentioned above.

Subsequently, we systematically investigated the reaction conditions using **Se1** and **G10** as catalysts, as summarized in Table 2. Notably, no desired product was observed when either the diaryldiselenide catalyst or the chiral guanidine catalyst was used alone (entries 2 and 3). The absence of a drying agent significantly decreased the yield of **3aa** from 86% to 63% (entry 4), and replacing 4 Å molecular sieves with $MgSO_4$ also led to a reduced yield (entry 5). These observations indicated that the presence of water significantly influenced the formation of **3aa**, although it did not affect the enantiocontrol of the reaction. A survey of solvents revealed that aromatic chlorinated solvents provided good yield and enantioselectivity. Switching from 2-chlorotoluene to chlorobenzene or toluene slightly decreased the yield of **3aa** (entries 6 and 7), while dichloromethane (DCM), 1,2-dichloroethane (DCE), and chloroform ($CHCl_3$) proved ineffective for this transformation (entries 8 and 9), Furthermore, the enantioselectivity was found to be highly sensitive to temperature, with the enantiomeric ratio (e.r.) of **3aa** decreasing as the temperature increased (entries 10 and 11). Although lower temperatures led to an improvement in enantioselectivity, the reaction only afforded a 60% yield (entry 12).

Substrates cope study

With the optimized reaction conditions established, we proceeded to evaluate the substrate scope of this novel reaction strategy. First, the scope of phosphine oxides was investigated. As shown in Scheme 1, a series of *para*-substituted phenyl rings, bearing either electron-donating or electron-withdrawing groups, afforded products (**3aa–3ah**) with excellent yields and enantiomeric excess (up to 97% yield and 97 : 3 e.r.). The absolute *S*-configuration of **3ga** was determined by X-ray crystallographic analysis (CCDC 2426084), and the configurations of the other products were assigned by analogy.

Notably, no product formation was observed with *ortho*-substituted phosphine oxides (**3ai**), which we attribute to significant steric hindrance that likely impedes the reaction between the phosphine oxide and diaryldiselenide. In contrast,

Table 2 Optimization of the reaction conditions[a]

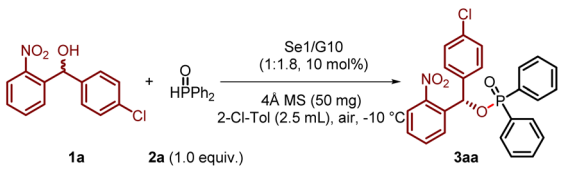

1a **2a** (1.0 equiv.) **3aa**

Entry	Variation from standard	Yield (%)	e.r. (%)
1	None	86	95 : 5
2	Without $(ArSe)_2$ catalyst	0	—
3	Without G10 catalyst	0	—
4	Without 4 Å MS	63	95 : 5
5	$MgSO_4$ instead of 4 Å MS	71	95 : 5
6	PhCl instead of 2-Cl-Tol	73	95.5 : 4.5
7	$PhCH_3$ instead of 2-Cl-Tol	56	95 : 5
8	DCM instead of 2-Cl-Tol	Trace	—
9	DCE or $CHCl_3$ instead of 2-Cl-Tol	0	—
10	rt instead of −10 °C	83	88 : 12
11	0 °C instead of −10 °C	85	93 : 7
12	−20 °C instead of −10 °C	60	96 : 4

[a] **1a** (0.25 mmol), **2a** (0.1 mmol), **Se1** (10 mol%), **G10** (18 mol%), 4 Å MS (50 mg), 2-Cl-Tol (2.5 mL), −10 °C, air. The yields given are isolated yields (based on **2a**). Enantiomeric ratio (e.r.) was determined by HPLC analysis.

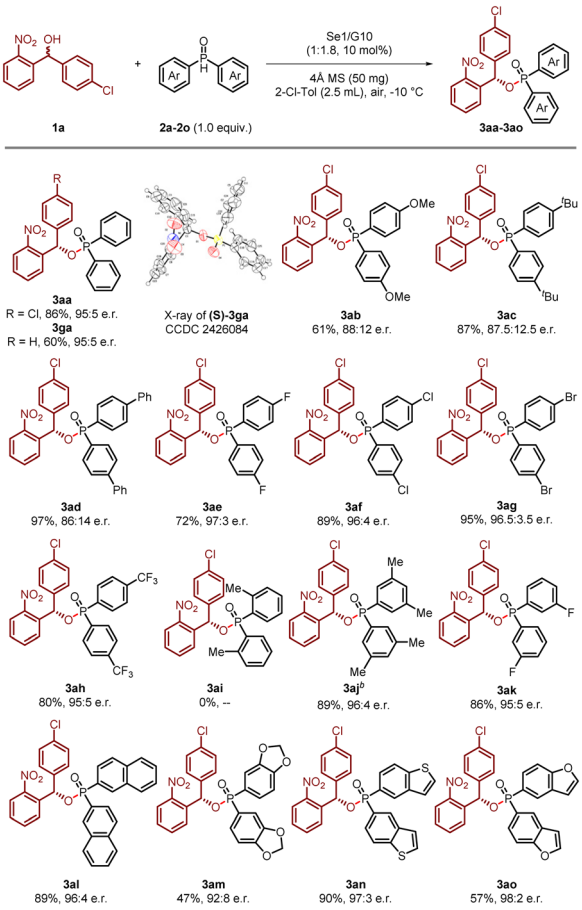

Scheme 1 Scope of phosphine oxides[a]. [a]Reaction conditions: **1a** (0.25 mmol), **2a-2o** (0.1 mmol), **Se1** (10 mol%), **G10** (18 mol%), 4 Å MS (50 mg), 2-Cl-Tol (2.5 mL), −10 °C, air. The yields given are isolated yields (based on **2**). Enantiomeric ratio (e.r.) was determined by HPLC analysis. [b]The $MgSO_4$ as drying agent instead of 4 Å MS.

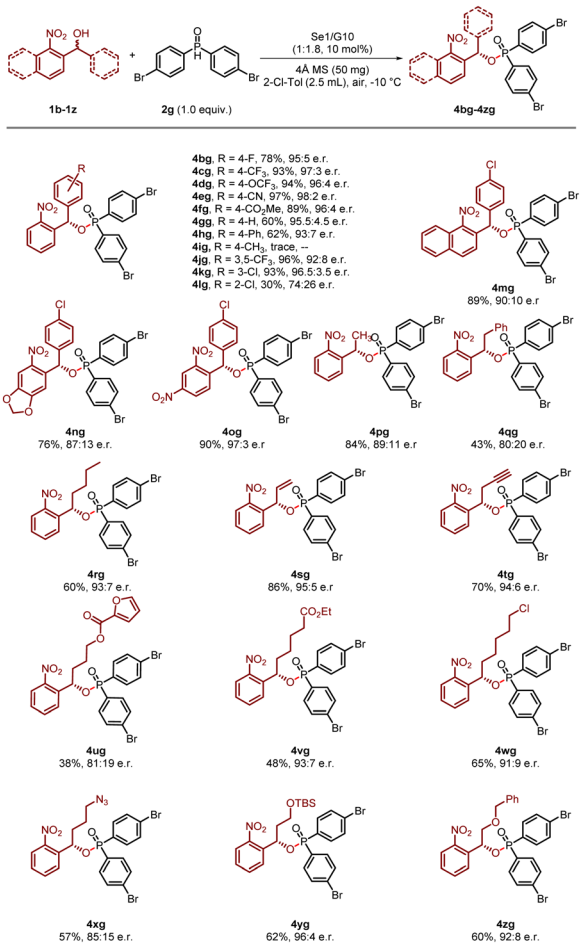

Scheme 2 Scope of 2-nitrobenzhydrols[a]. [a]Reaction conditions: **1b–1z** (0.25 mmol), **2g** (0.1 mmol), **Se1** (10 mol%), **G10** (18 mol%), 4 Å MS (50 mg), 2-Cl-Tol (2.5 mL), −10 °C, air. The yields given are isolated yields (based on **2g**). Enantiomeric ratio (e.r.) was determined by HPLC analysis.

meta-substituted phosphine oxides proved to be excellent substrates, delivering the desired phosphinate products (**3aj** and **3ak**) in high yields with exceptional enantiocontrol. Additionally, β-naphthyl phosphine oxide demonstrated remarkable reactivity, affording the desired compound **3al** in 89% yield with 96 : 4 enantiomeric ratio (e.r.). Furthermore, phosphine oxides incorporating heteroaromatic moieties, such as benzodioxole (**3am**), benzothiophene (**3an**) and benzofuran (**3ao**), were also found to be excellent substrates, yielding the corresponding products in moderate to high yields with consistently high enantioselectivity.

Subsequently, we further explored the scope of 2-nitrobenzhydrols. As shown in Scheme 2, a diverse range of substrates containing strong electron-withdrawing groups (F, Cl, CF_3, OCF_3, CN, CO_2Me) at the *para* position of the phenyl ring were successfully transformed into the desired products (**4bg–4fg**), achieving high yields (78–97%) along with remarkable enantiomeric excess values (95 : 5–98 : 2 e.r.). This high performance highlights the beneficial role of electron-withdrawing groups in enhancing both reactivity and stereocontrol. In contrast, substrates featuring an unsubstituted benzene ring (**4gg**) and biphenyl (**4hg**) showed a moderate reduction in both yield and enantiomeric excess, further supporting the importance of electron-withdrawing groups. Consistent with this trend, substrates containing methyl (Me) substituents yielded only trace amounts of product (**4ig**). Additionally, substrates with *meta*-substituents on the aryl unit also afforded the desired products, **4jg** and **4kg**, in excellent yields with good to excellent enantiomeric excess values. However, the substrate bearing a sterically demanding *ortho*-Cl substituent produced the desired product (**4lg**) in only 30% yield with 74 : 26 enantiomeric ratio (e.r.). Furthermore, substitution patterns on the nitrobenzene ring were well tolerated under the standard reaction conditions (**4mg–4og**), suggesting flexibility in this moiety. Notably, the methodology was further evaluated using substrates containing alkyl groups of varying chain lengths as well as functionalized moieties, including terminal alkenyl, alkyne, unactivated ester, primary alkyl chloride/azide, and silyl/benzyl ether, which proved effective in the formation of chain tertiary carbon stereocenters in good yield and enantioselectivity (**4pg–4zg**).

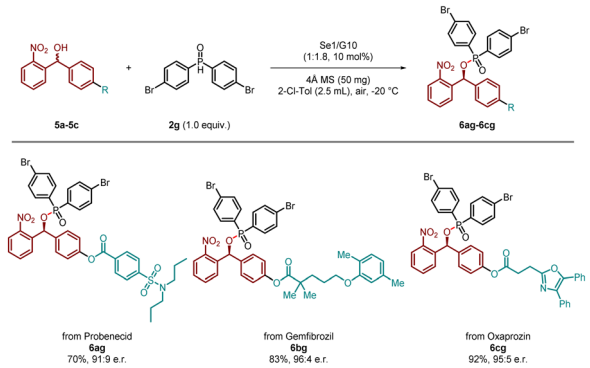

Scheme 3 Late-stage modification of complex molecule substrate scope[a] [a]reaction conditions: **5a–5c** (0.25 mmol), **2g** (0.1 mmol), **Se1** (10 mol%), **G10** (18 mol%), 4 Å MS (50 mg), 2-Cl-Tol (2.5 mL), −20 °C, air. The yields given are isolated yields (based on **2g**). Enantiomeric ratio (e.r.) was determined by HPLC analysis.

For the purpose of further validating the synthetic utility of this methodology, we extended the substrate scope to investigate its application in the late-stage functionalization of natural products and drug molecules (Scheme 3). Encouragingly, 2-nitrobenzhydrol derivatives derived from probenecid, gemfibrozil, and oxaprozin were successfully transformed into the corresponding phosphinates (**6ag**, 70%, 91 : 9 e.r.; **6bg**, 83%, 96 : 4 e.r.; **6cg**, 92%, 95 : 5 e.r.) with excellent yields and enantioselectivities. Although the substrate scope was relatively broad with respect to the other substituent of the secondary alcohol, the requirement that one substituent on the alcohol must be an *ortho*-nitrophenyl group imposed a limitation on the scope.

Scale-up experiments and synthetic application

To further demonstrate the synthetic potential of this synergistic catalytic system, the reaction was successfully scaled up to 2 mmol, providing compounds **3ag** and **3ga** in excellent yields and enantioselectivities (**3ag**, 90%, 96.5 : 3.5 e.r.; **3ga**, 54%, 95 : 5 e.r.). The enantiomeric ratio was further improved after recrystallization (**3ag**, 81%, >99.5 : 0.5 e.r.; **3ga**, 43%, 98.5 : 1.5 e.r.; Scheme 4A). The enantioenriched phosphinate **3ga** could be efficiently reduced to form chiral 2-nitrobenzhydrol **7** (84%, 97 : 3 e.r.), which exhibited potential for the development of innovative antibacterial therapies.[16] Particularly practicable is the facile conversion of compound **7** into a diverse range of functionalized molecules (Scheme 4B). Initially, the direct acylation of **7** afforded hydroxyl-protected derivative **8** with 87% yield and 97 : 3 enantiomeric ratio (e.r.). Significantly, this structurally well-defined compound **8** serves as a versatile coupling reagent, demonstrating functionality as a key synthetic intermediate. Subsequently, the reduction of the nitro group was achieved using $NaBH_4/NiCl_2\cdot 6H_2O$, which smoothly delivered the corresponding chiral amino-alcohol derivatives **9** with complete retention of configuration. Furthermore, the stereospecific Mitsunobu reaction of the secondary alcohol was successfully achieved under optimized conditions (DEAD, PPh_3, THF, 0 °C), yielding configurationally inverted chiral azide **10**

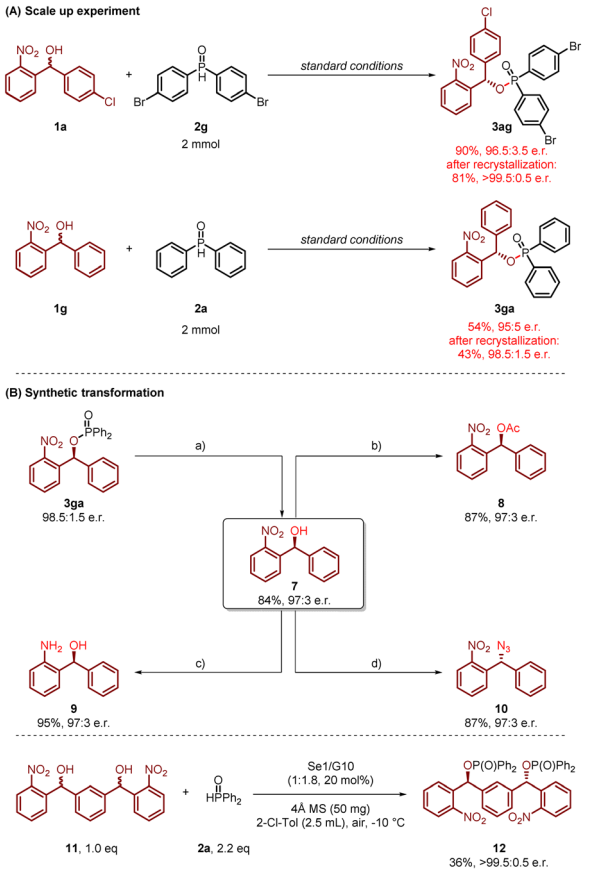

Scheme 4 Transformations and applications[a]. [a]Reaction conditions: (a) $LiAlH_4$ (5.0 equiv.), THF, 0 °C, 30 min; (b) CH_3COCl (1.2 equiv.), Et_3N (1.5 equiv.), DCM, rt; (c) $NaBH_4$ (10.0 equiv.), $NiCl_2\cdot 6H_2O$ (1.0 equiv.), EtOH, 0 °C; (d) diphenylphosphoryl azide (1.2 equiv.), DEAD (2.0 equiv.), PPh_3 (2.0 equiv.), THF, 0 °C.

with 87% yield and 97 : 3 enantiomeric ratio (e.r.). The isophthalaldehyde-derived compound **11** undergoes efficient bisphosphorylation under standard conditions, affording the corresponding bisphosphorus compound **12** with 36% yield and 99.5 : 0.5 enantiomeric ratio (e.r.). This product serves as a promising precursor for the synthesis of a chiral PCP pincer type ligands, which have demonstrated significant potential in transition metal catalysis. However, it's a pity that the reaction exhibits limited diastereoselectivity (dr = 1 : 1.5).

Mechanistic studies

To gain insight into the reaction mechanism, we prepared the P(O)-SeAr intermediate A *in situ* from **2a** and **Se1**, which was identified by HRMS ($[M + H]^+$ *m*/*z* 494.9838). The ^{31}P and ^{77}Se NMR spectra of intermediate A each exhibited a doublet with coupling constants of identical magnitude ($^1J_{PSe} = -346$ Hz), consistent with the formation of a P–Se bond in **Int-A**.[19] (Scheme 5A). After that, we used **Int-A** as the starting material to carry out the model reaction, which afforded the target product **3aa** in 56% yield with 96 : 4 enantiomeric ratio (e.r.) (Scheme 5B(a)). In contrast, only a trace amount of **3aa** was detected in the absence of **G10** (Scheme 5B(b)). These results indicate that the chiral

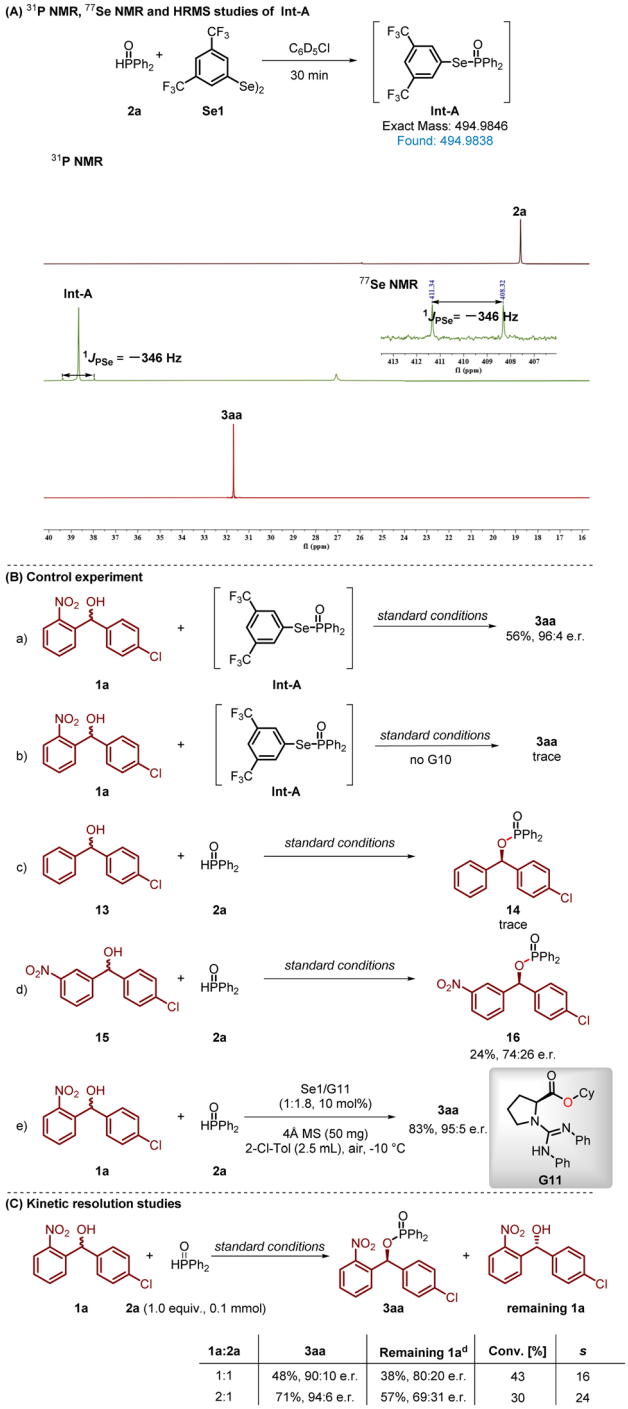

1a:2a	3aa	Remaining 1a[d]	Conv. [%]	s
1:1	48%, 90:10 e.r.	38%, 80:20 e.r.	43	16
2:1	71%, 94:6 e.r.	57%, 69:31 e.r.	30	24

Scheme 5 Mechanistic studies.

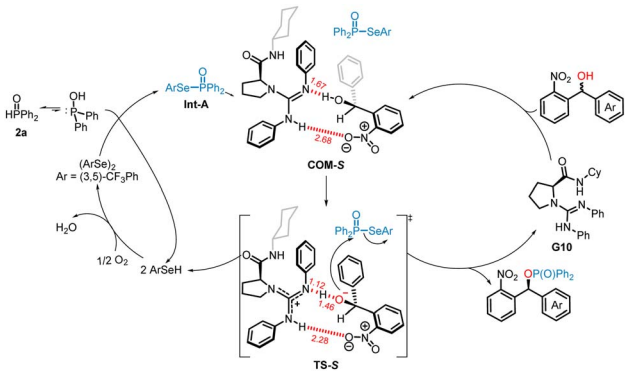

Scheme 6 Proposed catalytic cycle.

organo-superbase catalyst **G10** is responsible for deprotonating secondary alcohols in this transformation. Further control experiments were performed to explore the impact of structural modifications. Under the standard reaction conditions, substrates without nitro groups (**13**) exhibited remarkably low reactivity, affording only trace amounts of the desired product **14** (Scheme 5B(c)). This pronounced substrate effect was further corroborated when the nitro group was placed at the 3-position (**15**), resulting in significantly diminished reaction efficiency and enantioselectivity (**16**, 24%, 74 : 26 e.r.) (Scheme 5B(d)). These results demonstrate that the nitro group, serving as a strong hydrogen-bond acceptor, significantly enhances the reactivity and enantioselective control. Comparative experiments were executed with the O derivative (**G11**) of the corresponding guanidine catalyst **G10**. Notably, the enantioselectivity stayed consistent under the same reaction conditions, suggesting the N–H moiety of the amide in the catalyst does not contribute to the regulation of enantioselectivity (Scheme 5B(e)). With the facts that the product enantiomeric ratio was influenced by the amount of alcohol and racemic 2-nitrobenzhydrols were employed in this dehydrophosphorylation reaction, we proposed that the reaction proceeds *via* a kinetic resolution process.[20] To verify this hypothesis, some control experiments were conducted (see Scheme 5C, 5B). The reaction with 0.2 mmol of racemic alcohol **1a** and 0.1 mmol of **2a** was carried out under standard reaction conditions, **3aa** was obtained in 71% yield and 94 : 6 e.r. (based on **2a**), and the unreacted alcohol was recovered in a 57% yield with 69 : 31 e.r. (based on **1a**). When equal amounts of **1a** and **2a** were used, **3aa** was obtained in 48% yield with 90 : 10 e.r. (based on **2a**), accompanied by the unreacted **1a** being left with a 38% yield and 80 : 20 e.r. (based on **1a**). These experimental results demonstrate that racemic alcohol **1a** should go through a kinetic resolution in this synergistic catalysis protocol.

Based on the above experiments and literature reports,[11g,17d,e,21] a plausible mechanism is proposed for this transformation, as illustrated in Scheme 6. The catalytic variant of the Atherton–Todd reaction enables the coupling of two formally nucleophilic reagents *via* a three-step process: (1) selenophosphorylation of the phosphorus substrate: the nucleophilic P(O)–H compound reacts rapidly with the diaryldiselenide to form P(O)-SeAr intermediate **A**, accompanied by the release of arylselenol. (2) Chiral guanidine catalyst **G10** enables kinetic resolution of the racemic alcohol: density functional theory (DFT) calculations (Fig. S1–S3 in SI for details) indicate that the second step involves a concerted mechanism. When **G10** interacts with **Int-A** and the substrate (*S*)-2-nitrobenzhydrol, molecular complex **COM-*S*** is formed; after which, the hydroxyl proton of the (*S*)-2-nitrobenzhydrol transfers to the catalyst, while the chiral alkoxide ion undergoes

nucleophilic substitution at the P(O)-SeAr intermediate *via* the transition state **TS-*S***, affording the P(O)-Nu product alongside the liberation of arylselenol and regeneration of the chiral guanidine catalyst. IGMH analysis of **TS-*S*** (Fig. S4 in SI) revealed that during the proton transfer process, the hydroxyl proton exhibits a distinct tendency to form an N–H bond with the catalyst, with a considerable degree of covalent character observed in this interaction. Simultaneously, there is a strong bonding tendency between the hydroxyl oxygen atom and the phosphorus atom. The system is further stabilized by various significant weak interactions, including π–π stacking and C–H···π interactions. (3) Regeneration of the diselenide catalyst: The liberated arylselenol intermediate undergoes aerobic oxidation under air conditions, regenerating the diaryldiselenide catalyst and completing the catalytic cycle.

Conclusions

In conclusion, we have developed an efficient catalytic system for the dehydrophosphorylation of 2-nitrobenzhydrols with P(O)–H compounds through the synergistic action of diselenide and guanidine catalysts. The strategy leverages both the unique reactivity of the diaryldiselenide catalyst to activate P(O)–H bonds and the role of chiral guanidine to resolve secondary alcohols, offering a sustainable and efficient route to C-stereogenic phosphinates. The reaction proceeds under mild conditions, providing access to a diverse range of enantio-enriched phosphinates with excellent functional group tolerance, and the resulting chiral phosphinates serve as versatile synthetic intermediates for further transformations. A limitation of the current system is that one substituent on the alcohol must be an *ortho*-nitrophenyl group. Further exploration of this catalytic strategy is in progress in our group, with the aim of synthesizing other important P-chirogenic compounds and broadening its utility in synthetic organic chemistry.

Author contributions

Methodology, S.-D. Y.; investigation, J.-Y. G., Z.-C. Q. and Q.-X. F.; computational studies, P.-P. Z. and Y.-H. Q.; writing – original draft, S.- D. Y., J.-Y. G. and P.-P. Z.; writing – review & editing, S.-D. Y., J.-Y. G., Z.-C. Q., Q.-M. Z., Y.-H. Q. and P.-P. Z.; supervision, S.-D. Y.

Conflicts of interest

There are no conflicts to declare.

Data availability

CCDC 2426084 contains the supplementary crystallographic data for this paper.[22]

All experimental procedures, characterisation data, mechanistic investigations, NMR spectra and HPLC spectra can be found in the supplementary information (SI). Supplementary information: general information, experimental procedures and characterization data of the synthesized compounds. See DOI: https://doi.org/10.1039/d5sc07228j.

Acknowledgements

We are grateful to the NSFC (No. 22171119 and 22371105) and The Science and Technology Major Program of Gansu Province of China (22ZD6FA006, 23ZDFA015, 24ZD13FA017) for financial support.

Notes and references

1 (*a*) Ł. Joachimiak and K. M. Błażewska, *J. Med. Chem.*, 2018, **61**, 8536–8562; (*b*) A. Babbs, A. Berg, M. Chatzopoulou, K. E. Davies, S. G. Davies, B. Edwards, D. J. Elsey, E. Emer, S. Guiraud, S. Harriman, C. Lecci, L. Moir, D. Peters, N. Robinson, J. A. Rowley, A. J. Russell, S. E. Squire, J. M. Tinsley, F. X. Wilson and G. M. Wynne, *J.Med. Chem.*, 2020, **63**, 7880–7891.

2 M. Eto, *Biosci., Biotechnol., Biochem.*, 1997, **61**, 1–11.

3 (*a*) J.-L. Montchamp, *Acc. Chem. Res.*, 2014, **47**, 77–87; (*b*) G.-J. Wu, D.-X. Tan and F.-S. Han, *Acc. Chem. Res.*, 2021, **54**, 4354–4370.

4 For the application of the Atherton–Todd reaction in phosphorylation, see: (*a*) F. R. Atherton, H. T. Openshaw and A. R. Todd, *J. Chem. Soc.*, 1945, 660–663; (*b*) F. R. Atherton and A. R. Todd, *J. Chem. Soc.*, 1947, 674–678; (*c*) E. M. Georgiev, J. Kaneti, K. Troev and D. M. Roundhill, *J. Am. Chem. Soc.*, 1993, **115**, 10964–10973; (*d*) G. Wang, R. Shen, Q. Xu, M. Goto, Y. Zhao and L.-B. Han, *J. Org. Chem.*, 2010, **75**, 3890–3892; (*e*) S. Wagner, M. Rakotomalala, Y. Bykov, O. Walter and M. Döring, *Heteroat. Chem.*, 2012, **23**, 216–222; (*f*) S. Li, T. Chen, Y. Saga and L.-B. Han, *RSC Adv.*, 2015, **5**, 71544–71546; (*g*) B. Kaboudin, F. Kazemi and F. Habibi, *Tetrahedron Lett.*, 2015, **56**, 6364–6367; (*h*) Q. Chen, J. Zeng, X. Yan, Y. Huang, C. Wen, X. Liu and K. Zhang, *J. Org. Chem.*, 2016, **81**, 10043–10048; (*i*) P. A. Volkov, K. B. Petrushenko, N. I. Ivanova, K. O. Khrapova, L. I. Larina, N. K. Gusarova and B. A. Trofimov, *Tetrahedron Lett.*, 2017, **58**, 1992–1995; (*j*) J. Eljo and G. K. Murphy, *Tetrahedron Lett.*, 2018, **59**, 2965–2969; (*k*) Y. Ou, Y. Huang, Z. He, G. Yu, Y. Huo, X. Li, Y. Gao and Q. Chen, *Chem. Commun.*, 2020, **56**, 1357–1360; (*l*) X. Yu, S. Zhang, Z. Jiang, H.-S. Zhang and T. Wang, *Eur. J. Org Chem.*, 2020, **2020**, 3110–3113; (*m*) S. Zhao, Y. Guo, Z. Su, C. Wu, W. Chen and Q.-Y. Chen, *Chin. J. Chem.*, 2021, **39**, 1225–1232; (*n*) Y. Tan, Y.-P. Han, Y. Zhang, H.-Y. Zhang, J. Zhao and S.-D. Yang, *J. Org. Chem.*, 2022, **87**, 3254–3264; (*o*) S. Fang, Z. Liu, Z. Su and T. Wang, *ACS Catal.*, 2025, **15**, 9660–9671.

5 For the iodide-mediated dehydrophosphorylation, see: (*a*) J. Dhineshkumar and K. R. Prabhu, *Org. Lett.*, 2013, **15**, 6062–6065; (*b*) J. Wang, X. Huang, Z. Ni, S. Wang, J. Wu and Y. Pan, *Green Chem.*, 2015, **17**, 314–319; (*c*) T. Anitha, K. C. Ashalu, M. Sandeep, A. Mohd, J. Wencel-Delord, F. Colobert and K. R. Reddy, *Eur. J. Org Chem.*, 2019, **2019**, 7463–7474; (*d*) X. Wang, Y. Ou, Z. Peng, G. Yu, Y. Huang,

X. Li, Y. Huo and Q. Chen, *J. Org. Chem.*, 2019, **84**, 14949–14956; (*e*) C. Tan, X. Liu, H. Jia, X. Zhao, J. Chen, Z. Wang and J. Tan, *Chem. -Eur. J.*, 2020, **26**, 881–887.

6 For the Tf_2O-mediated dehydrophosphorylation, see: (*a*) Y. Unoh, K. Hirano and M. Miura, *J. Am. Chem. Soc.*, 2017, **139**, 6106–6109; (*b*) T. Yuan, S. Huang, C. Cai and G.-P. Lu, *Org. Biomol. Chem.*, 2018, **16**, 30–33; (*c*) J. Shen, Q.-W. Li, X.-Y. Zhang, X. Wang, G.-Z. Li, W.-Z. Li, S.-D. Yang and B. Yang, *Org. Lett.*, 2021, **23**, 1541–1547; (*d*) H.-Q. Yue, D.-W. Shi, M. Li, S.-Q. Gao, M.-X. Sun, S. Zhang, S.-D. Yang and B. Yang, *Chem. Commun.*, 2023, **59**, 10817–10820; (*e*) H.-Q. Yue, D.-W. Shi, P. Zhang, B. Xiao, L.-T. Jia, R. Li, S.-N. Zhao, S.-D. Yang and B. Yang, *Org. Lett.*, 2024, **26**, 8939–8944; (*f*) D.-W. Shi, H.-Q. Yue, M. Li, J. Liu, C.-C. Wang, S.-D. Yang and B. Yang, *J. Org. Chem.*, 2024, **89**, 6729–6739; (*g*) D.-W. Shi, M. Li, R.-J. Yang, X.-Y. Zhao, T. Zhang, J. Huangfu, L. Xu, K. Wang, Y.-X. Ma and B. Yang, *J. Org. Chem.*, 2025, **90**, 5578–5585.

7 A. Mohd, T. Anitha, K. R. Reddy, J. Wencel-Delord and F. Colobert, *Eur. J. Org Chem.*, 2019, **2019**, 7836–7841.

8 (*a*) S. Fang, J.-P. Tan, J. Pan, H. Zhang, Y. Chen, X. Ren and T. Wang, *Angew. Chem., Int. Ed.*, 2021, **60**, 14921–14930; (*b*) J. He, X. Luo, S. Fang, Z. Su, C. Hu and T. Wang, *Org. Chem. Front.*, 2025, **12**, 3389–3402.

9 S. Fang, Z. Liu, H. Zhang, J. Pan, Y. Chen, X. Ren and T. Wang, *ACS Catal.*, 2021, **11**, 13902–13912.

10 S. Fang, J. He, Z. Liu, Z. Su, F. Guo and T. Wang, *ACS Catal.*, 2023, **13**, 13077–13088.

11 Selenium-catalyzed organic reactions: (*a*) T. Hori and K. B. Sharpless, *J. Org. Chem.*, 1979, **44**, 4204–4208; (*b*) S. R. Mellegaard and J. A. Tunge, *J. Org. Chem.*, 2004, **69**, 8979–8981; (*c*) S. K. Bhunia, P. Das and R. Jana, *Org. Biomol. Chem.*, 2018, **16**, 9243–9250; (*d*) J. Wang, X. Wang, H. Li and J. Yan, *J. Organomet. Chem.*, 2018, **859**, 75–79; (*e*) C. Depken, F. Krätzschmar, R. Rieger, K. Rode and A. Breder, *Angew. Chem., Int. Ed.*, 2018, **57**, 2459–2463; (*f*) R. Choudhary, P. Singh, R. Bai, M. C. Sharma and S. S. Badsara, *Org. Biomol. Chem.*, 2019, **17**, 9757–9765; (*g*) Handoko, Z. Benslimane and P. S. Arora, *Org. Lett.*, 2020, **22**, 5811–5816; (*h*) S.-i. Fukuzawa, K. Takahashi, H. Kato and H. Yamazaki, *J. Org. Chem.*, 1997, **62**, 7711–7716; (*i*) T. Wirth, S. Häuptli and M. Leuenberger, *Tetrahedron: Asymmetry*, 1998, **9**, 547–550; (*j*) M. Tiecco, L. Testaferri, C. Santi, C. Tomassini, F. Marini, L. Bagnoli and A. Temperini, *Tetrahedron: Asymmetry*, 2000, **11**, 4645–4650; (*k*) D. M. Browne, O. Niyomura and T. Wirth, *Org. Lett.*, 2007, **9**, 3169–3171; (*l*) Y. Kawamata, T. Hashimoto and K. Maruoka, *J. Am. Chem. Soc.*, 2016, **138**, 5206–5209; (*m*) Z. Tao, B. B. Gilbert and S. E. Denmark, *J. Am. Chem. Soc.*, 2019, **141**, 19161–19170; (*n*) J. E. Tungen, R. Kristianslund, A. Vik and T. V. Hansen, *J. Org. Chem.*, 2019, **84**, 11373–11381; (*o*) E. M. Mumford, B. N. Hemric and S. E. Denmark, Catalytic, *J. Am. Chem. Soc.*, 2021, **143**, 13408–13417; (*p*) C. C. Cunningham, J. L. Panger, M. Lupi and S. E. Denmark, *Org. Lett.*, 2024, **26**, 6703–6708.

12 (*a*) D. M. Freudendahl, S. Santoro, S. A. Shahzad, C. Santi and T. Wirth, *Angew. Chem., Int. Ed.*, 2009, **48**, 8409–8411; (*b*) S. Ortgies and A. Breder, *ACS Catal.*, 2017, **7**, 5828–5840; (*c*) L. Shao, Y. Li, J. Lu and X. Jiang, *Org.Chem.Front.*, 2019, **6**, 2999–3041; (*d*) V. Rathore, C. Jose and S. Kumar, *New J. Chem.*, 2019, **43**, 8852–8864; (*e*) H. Cao, R. Qian and L. Yu, *Catal. Sci. Technol.*, 2020, **10**, 3113–3121; (*f*) L. Liao and X. Zhao, *Chem. Lett.*, 2021, **50**, 1104–1113; (*g*) W.-M. Wang, L.-J. Liu, L. Yao, F.-J. Meng, Y.-M. Sun, C.-Q. Zhao, Q. Xu and L.-B. Han, *J. Org. Chem.*, 2016, **81**, 6843–6847; (*h*) S. M. Akondi, P. Gangireddy, T. C. Pickel and L. S. Liebeskind, *Org. Lett.*, 2018, **20**, 538–541; (*i*) T. C. Pickel, S. M. Akondi and L. S. Liebeskind, *J. Org. Chem.*, 2019, **84**, 4954–4960; (*j*) S. S. Handoko, N. R. Panigrahi and P. S. Arora, *J. Am. Chem. Soc.*, 2019, **141**, 15977–15985; (*k*) N. R. P. Handoko and P. S. Arora, *J. Am. Chem. Soc.*, 2022, **144**, 3637–3643; (*l*) L. Liao and X. Zhao, *Synlett*, 2021, **32**, 1262–1268; (*m*) W. Qiu, L. Liao, X. Xu, H. Huang, Y. Xu and X. Zhao, *Nat. Commun.*, 2024, **15**, 3632; (*n*) J. Y. See, H. Yang, Y. Zhao, M. W. Wong, Z. Ke and Y.-Y. Yeung, *ACS Catal.*, 2018, **8**, 850–858; (*o*) H.-Y. Luo, Z.-H. Li, D. Zhu, Q. Yang, R.-F. Cao, T.-M. Ding and Z.-M. Chen, *J. Am. Chem. Soc.*, 2022, **144**, 2943–2952; (*p*) R.-F. Cao, Z.-W. Wei, S.-K. Li, T.-M. Ding, H. Ke and Z.-M. Chen, *Chem. Commun.*, 2025, **61**, 8532–8535; (*q*) R.-F. Cao, R. Su, Z.-W. Wei, Z.-L. Li, D. Zhu, Y.-X. Huo, X.-S. Xue and Z.-M. Chen, *Nat. Commun.*, 2025, **16**, 2147.

13 Z.-C. Qi, Y. Li, J. Wang, L. Ma, G.-W. Wang and S.-D. Yang, *ACS Catal.*, 2023, **13**, 13301–13309.

14 (*a*) S.-X. Li, Y.-N. Ma and S.-D. Yang, *Org. Lett.*, 2017, **19**, 1842–1845; (*b*) Y.-N. Ma, S.-X. Li and S.-D. Yang, *Acc. Chem. Res.*, 2017, **50**, 1480–1492; (*c*) X. Zhang, J. Wang and S.-D. Yang, *ACS Catal.*, 2021, **11**, 14008–14015; (*d*) S. Ying, X. Huang, X. Guo and S. Yang, *Green Synth. Catal.*, 2021, **2**, 315–319.

15 Some Reviews of Chiral organo-superbases: (*a*) T. Ishikawa, *Superbases for organic synthesis: guanidines, amidines and phosphazenes and related organocatalysts*, Wiley Online Library, 2009; (*b*) X. Liu, L. Lin and X. Feng, *Chem. Commun.*, 2009, 6145–6158; (*c*) J. E. Taylor, S. D. Bull and J. M. J. Williams, *Chem. Soc. Rev.*, 2012, **41**, 2109–2121; (*d*) H. Krawczyk, M. Dzięgielewski, D. Deredas, A. Albrecht and Ł. Albrecht, *Chem. -Eur. J.*, 2015, **21**, 10268–10277; (*e*) B. Teng, W. C. Lim and C.-H. Tan, *Synlett*, 2017, **28**, 1272–1277; (*f*) W. Cao, X. Liu and X. Feng, *Chin. Chem. Lett.*, 2018, **29**, 1201–1208; (*g*) M. Formica, D. Rozsar, G. Su, A. J. M. Farley and D. J. Dixon, *Acc. Chem. Res.*, 2020, **53**, 2235–2247; (*h*) Y.-H. Wang, Z.-Y. Cao, Q.-H. Li, G.-Q. Lin, J. Zhou and P. Tian, *Angew. Chem., Int. Ed.*, 2020, **59**, 8004–8014; (*i*) K. Vazdar, D. Margetić, B. Kovačević, J. Sundermeyer, I. Leito and U. Jahn, *Acc. Chem. Res.*, 2021, **54**, 3108–3123.

16 M. P. Storz, G. Allegretta, B. Kirsch, M. Empting and R. W. Hartmann, *Org. Biomol. Chem.*, 2014, **12**, 6094–6104.

17 For selected examples of chiral guanidines and their derivatives in enantioselective reactions, see: (*a*) D. Leow and C.-H. Tan, *Asian J.*, 2009, **4**, 488–507; (*b*) X. Fu and C.-H. Tan, *Chem. Commun.*, 2011, **47**, 8210–8222; (*c*) Y. Yang, S. Dong, X. Liu, L. Lin and X. Feng, *Chem.*

Commun., 2012, **48**, 5040–5042; (*d*) L. Wu, G. Li, Q. Fu, L. Yu and Z. Tang, *Org. Biomol. Chem.*, 2013, **11**, 443–447; (*e*) T. Kang, P. Zhao, J. Yang, L. Lin, X. Feng and X. Liu, *Chem. -Eur. J.*, 2018, **24**, 3703–3706; (*f*) S. Dong, X. Feng and X. Liu, *Chem. Soc. Rev.*, 2018, **47**, 8525–8540; (*g*) H.-C. Chou, D. Leow and C.-H. Tan, *Chem.–Asian J.*, 2019, **14**, 3803–3822; (*h*) S. Ruan, X. Zhong, Q. Chen, X. Feng and X. Liu, *Chem. Commun.*, 2020, **56**, 2155–2158; (*i*) Y. Li, H. Pan, W.-Y. Li, X. Feng and X. Liu, *Synlett*, 2020, **32**, 587–592; (*j*) J. Li, Y. Mo, L. Yan, X. Feng, Z. Su and X. Liu, *CCS Chem.*, 2021, **4**, 650–659; (*k*) Q. Tan, N. Guo, L. Yang, F. Wang, X. Feng and X. Liu, *J. Org. Chem.*, 2023, **88**, 9332–9342; (*l*) P. Ruan, C. Zhang, J. Wu, F. Xiao, Y. Zhang, Q. Tan, Z. Su, X. Feng and X. Liu, *Chem. Commun.*, 2023, **59**, 8250–8253; (*m*) S. Li, C. Zhang, G. Pan, L. Yang, Z. Su, X. Feng and X. Liu, *ACS Catal.*, 2023, **13**, 4656–4666; (*n*) Y. Zhang, L. Ning, T. Zhu, Z. Xie, S. Dong, X. Feng and X. Liu, *Org. Chem. Front.*, 2024, **11**, 2897–2904; (*o*) X. He, Y. Fu, R. Xi, C. Zhang, K. Lan, Z. Su, F. Wang, X. Feng and X. Liu, *Angew. Chem., Int. Ed.*, 2025, **64**, e202417636.

18 For selected examples of the Resolution of Racemic alcohol Derivatives Catalyzed by Chiral Guanidine, see: (*a*) K. Nakata and I. Shiina, *Org. Biomol. Chem.*, 2011, **9**, 7092–7096; (*b*) S. Yoshimatsu, A. Yamada and K. Nakata, *J. Org. Chem.*, 2018, **83**, 452–458; (*c*) S. Yoshimatsu and K. Nakata, *Adv. Synth. Catal.*, 2019, **361**, 4679–4684; (*d*) T. Ichimura, R. Kishida and K. Nakata, *ChemistrySelect*, 2019, **4**, 9440–9443; (*e*) T. Suzuki, M. Iwakura and K. Nakata, *ChemistrySelect*, 2021, **6**, 11261–11264; (*f*) M. Iwakura, T. Ikeue and K. Nakata, *ChemistrySelect*, 2022, **7**, e202202511; (*g*) K. Miyazaki and K. Nakata, *J. Org. Chem.*, 2022, **87**, 10509–10515; (*h*) A. Ui, M. Iwakura, S. Yoshimatsu and K. Nakata, *Synlett*, 2025, **36**, 279–283; (*i*) Y. Homma, T. Ikeue and K. Nakata, *Chin. J. Chem.*, 2025, **43**, 1553–1559.

19 H. Duddeck, *Prog. Nucl. Magn. Reson. Spectrosc.*, 1995, **27**, 1–323.

20 (*a*) W.-Q. Cai, Q. Wei and Q.-W. Zhang, *Org. Lett.*, 2022, **24**, 1258–1262; (*b*) C. Wang, X. Hu, C. Xu, Q. Ge, Q. Yang, J. Xiong and W.-L. Duan, *Angew. Chem., Int. Ed.*, 2023, **62**, e202300011; (*c*) Q. Dai, W. Li, Z. Li and J. Zhang, *J. Am. Chem. Soc.*, 2019, **141**, 20556–20564; (*d*) H.-R. Yang, X. Cheng, X. Chang, Z.-F. Wang, X.-Q. Dong and C.-J. Wang, *Chem. Sci.*, 2024, **15**, 10135–10145; (*e*) K. Tian, X.-Q. Dong and C.-J. Wang, *J. Am. Chem. Soc.*, 2025, **147**, 33288–33303.

21 (*a*) T. Okino, Y. Hoashi and Y. Takemoto, *J. Am. Chem. Soc.*, 2003, **125**, 12672–12673; (*b*) S. B. Tsogoeva, D. A. Yalalov, M. J. Hateley, C. Weckbecker and K. Huthmacher, *Eur. J. Org Chem.*, 2005, 4995–5000, DOI: 10.1002/ejoc.200500420; (*c*) J. Wang, H. Li, W. Duan, L. Zu and W. Wang, *Org. Lett.*, 2005, **7**, 4713–4716; (*d*) Y. Sohtome, Y. Hashimoto and K. Nagasawa, *Adv. Synth. Catal.*, 2005, **347**, 1643–1648; (*e*) C. Rabalakos and W. D. Wulff, *J. Am. Chem. Soc.*, 2008, **130**, 13524–13525; (*f*) C. Palacio and S. J. Connon, *Chem. Commun.*, 2012, **48**, 2849–2851; (*g*) B. Fang, X. Liu, J. Zhao, Y. Tang, L. Lin and X. Feng, *J. Org. Chem.*, 2015, **80**, 3332–3338; (*h*) X. Fang and C.-J. Wang, *Chem. Commun.*, 2015, **51**, 1185–1197; (*i*) S. Vera, A. García-Urricelqui, A. Mielgo and M. Oiarbide, *Eur. J. Org Chem.*, 2023, **26**, e202201254, DOI: 10.1002/ejoc.202201254; (*j*) M. Formica, T. Rogova, H. Shi, N. Sahara, B. Ferko, A. J. M. Farley, K. E. Christensen, F. Duarte, K. Yamazaki and D. J. Dixon, *Nat. Chem.*, 2023, **15**, 714–721; (*k*) H. Li, C. Zhang, C. Hu and Z. Su, *J. Org. Chem.*, 2025, **90**, 4633–4645.

22 CCDC 2426084: Experimental Crystal Structure Determination, 2026, DOI: 10.5517/ccdc.csd.cc2mfjsd.